

Characterisation of pulsed Carbon fiber illuminators for FIR instrument calibration

S. Henrot-Versillé, R. Cizeron, F. Couchot

LAL Bât 200

versille@lal.in2p3.fr, cizeron@lal.in2p3.fr, couchot@lal.in2p3.fr

Abstract

We manufactured pulsed illuminators emitting in the far infrared for the Planck-HFI bolometric instrument ground calibrations. Specific measurements have been conducted on these light sources, based on Carbon fibers, to understand and predict their properties. We present a modelisation of the temperature dependence of the thermal conductivity and the calorific capacitance of the fibers. A comparison between simulations and bolometer data is given, that shows the coherence of our model. Their small time constants, their stability and their emission spectrum pointing in the submm range make these illuminators a very usefull tool for calibrating FIR instruments.

1 Introduction

We have been studying Carbon fibers as illuminators for FIR instrument calibration between 2000 and 2005 with the specific goal of measuring the sum of the electrical and optical crosstalk ¹ of the Planck-HFI instrument[1][2]. Our requirements were threefold:

- to get a signal ranging up to a few pW detected on the Planck-HFI bolometers for the concerned frequencies (ranging from 100 to 857 GHz) including transmission efficiency of the cold optics horns and integration over the 30% wide frequency bands.

¹The optical crosstalk is caused by potential leakages between the different cryogenic stages of the optics facing the bolometers.

- to get a relatively small time constant (smaller than 10ms) and a reproducible signal in a pulsed regime, allowing to stack the measurements in order to increase the signal over noise ratio.
- to be able to "lighten" the fibers without introducing any parasitic signal due to EMI-EMC from the electrical pulse used to drive them.

We did fulfill these requirements. Even more, on the time constant issue, we did get better than expected results and the fibers were one of the sources used to characterise the time response of the instrument.

Since the carbon fibers are composite materials, no measurement of the particular properties of the ones we used have been made. We therefore focus in this paper on their characterisation. In part 2 we give the heat equation and the corresponding approximations made in this paper to analyse the fiber behaviour. Part 3 describes the experimental setup and in part 4 we present the measurements of the relation between resistance and temperature and the analysis that leads to the measurement of the thermal conductivity and the calorific capacitance. Part 5 describes the fiber modelisation and a comparison of simulation results with data.

2 General framework

2.1 Equations and assumptions

The modelisation of the carbon fiber behaviour relies on the one dimensionnal heat equation (along the fiber):

$$\frac{\partial}{\partial x}(\kappa S \frac{\partial T}{\partial x}) + \frac{\mu I^2}{S} = \rho C_p S \frac{\partial T}{\partial t} \quad (1)$$

where:

- κ is the thermal conductivity, C_p the calorific capacitance, μ the resistivity. We assume here that all these parameters do depend on temperature T .
- ρ the mass per unit of volum, and S the surface of a slice [4]. The resistance R is obtained through $\mu(T)$ integration along the length L of the fiber. For the fibers we used, $L \simeq 1mm$ and the diameter of a slice is 6 microns: a photography is shown on figure 1. This picture

also shows the way it is thermalised at each end on a kapton circuit through Ag lacquer contacts.

- The fiber is powered by a current (I) generator.
- The radiated power represents less than 1% of thermal losses, even in the worst case ², so it is neglected with respect to conduction.



Figure 1: Photography of one of the carbon fiber used for the Planck-HFI calibration: the diameter is $6\mu\text{m}$ and the length $\simeq 1$ mm.

2.2 Basic properties

The fiber is thermalised at each end at a temperature T_0 (cf. figure 1). In the steady state regime, and in the simplest case where no parameter exhibits any temperature dependence, Eq. (1) gives:

$$\kappa \frac{\partial^2 T}{\partial x^2} + \frac{RI^2}{LS} = 0 \quad (2)$$

leading to (the fiber center being the x axis origin):

$$T(x) = T_0 + \frac{RI^2}{2LS\kappa} \left(\frac{L^2}{4} - x^2 \right) . \quad (3)$$

and a mean temperature increase:

$$\Delta T_{mes} = \frac{1}{L} \int_{-L/2}^{L/2} (T(x) - T_0) dx = \frac{RI^2 L}{12\kappa S} . \quad (4)$$

²The fiber radiates about $10\mu\text{W}$ when heated at about 200K by 1V pulses, dissipating about 1mW Joule power.

When one stops heating the fiber, the system relaxes to the T_0 temperature, and the transient regime can be described by the generic Fourier expansion solution:

$$T(x, t) = T_0 + \sum_{k=0}^{\infty} \Delta T_0^k e^{(-t/\tau_k)} \cos((2k+1)\pi x/L), \quad (5)$$

where the time constants τ_k are given by:

$$\tau_k = \frac{\rho C_p L^2}{\kappa (2k+1)^2 \pi^2}, \quad (6)$$

the leading term being by far the $k=0$ component, which corresponds to the longest time constant:

$$\tau_0 = \frac{\rho C_p L^2}{\kappa \pi^2}. \quad (7)$$

The fiber time constant is then proportional to the square of its length. Therefore, smaller time constants may be obtained with shorter fibers, at the price of a flux loss. L should stay sizeable with the longest needed wavelength, since the fiber acts like an antenna.

For small values of I , ΔT_{mes} is small, and these formula apply even if κ varies with T . We use this approximation in the following.

Resistivity dependence with T can be treated analytically in the simplest case where $\kappa(T)$ is constant, assuming $\mu(T)$ varies linearly as:

$$\mu(T) = \mu_0 [1 - \alpha(T - T_0)], \quad (8)$$

then, Eq. (1) exact solution for the mean temperature increase in steady state regime reads[4]:

$$\Delta T_{mes} = \frac{1}{\alpha} \left[1 - \frac{1}{\frac{LI}{2S} \sqrt{\frac{\mu_0 \alpha}{\kappa}}} \tanh \left(\frac{LI}{2S} \sqrt{\frac{\mu_0 \alpha}{\kappa}} \right) \right]. \quad (9)$$

3 Experimental setups

The measurements described in the following sections have been performed within the Saturne cryostat³ providing us with a thermalisation temperature

³This cryostat at IAS-Orsay has been used for the calibration of the Planck-HFI instrument.

ranging from 300K to 1.7K (we took advantage of the cooling down of the setup). Two kind of data are analysed:

- resistance (or resistance variations) measurements at the edges of the fibers done using the dedicated electronics described below for different thermalisation temperatures and for small values of the current applied on the fibers.
- bolometers' data translated in terms of incident power for a thermalisation temperature around 2K and a wide range of current values.

3.1 Dedicated electronics description

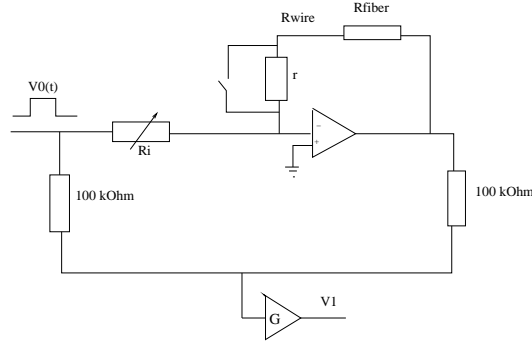


Figure 2: Figure illustrating the electronic circuit used to characterise the resistance of the carbon fibers.

The electronics used for resistance and resistance variation measurements is described in figure 2. The signal V_0 entering the circuit is a low impedance square signal which amplitude, frequency, and width can be changed. The output is simply given by:

$$V_1(t) = \left(1 - \frac{\tilde{R}_{tot}(t)}{R_i}\right)GV_0(t) \quad (10)$$

where \tilde{R}_{tot} corresponds to the resistance of the fiber in series with 15 meters long wires. Before any measurement we balance the system in order to get: $R_i \simeq \tilde{R}_{tot}(t = 0)$. Taking $t = 0$ at the beginning of the pulse, one gets:

$$V_1(t) = V_1(0) + \frac{GV_0(t)}{R_i}(R_{fiber}(t) - R_{fiber}(0)) \quad (11)$$

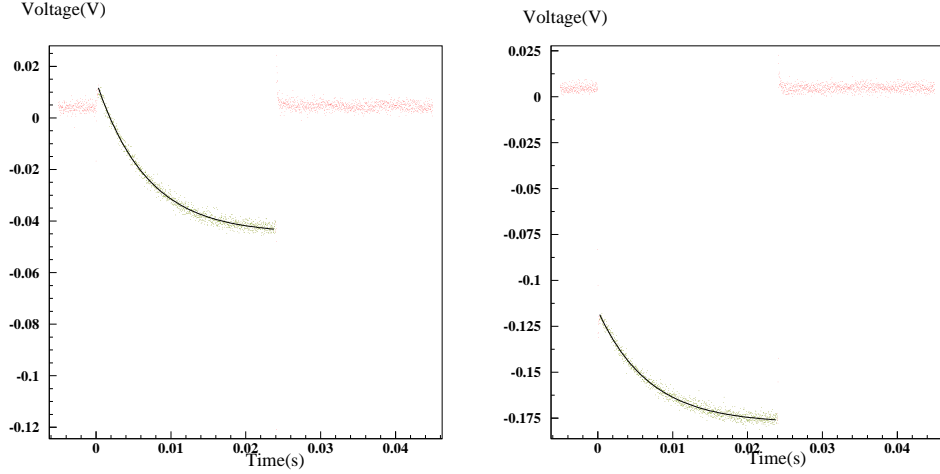


Figure 3: Example of $V_1(t)$ when a square signal V_0 of 0.2 V is applied: on the left when $r(\simeq 2.6\Omega)$ is switched on and on the right when it is off. The device reaches a precision of the order of $.05\Omega$ on the resistance variation measurements.

The gain factor is measured by switching on and off the small additional resistor r .

An example of the signal measured at the edges of the fibers is illustrated on figure 3 (cf. section 4.2.1 for more details).

3.2 Saturne setup

The setup of the fibers within the Saturne cryostat did take into account the constraints of all the measurements which were needed to be done to calibrate the Planck-HFI instrument (and which are not discussed here[3]). The fibers were therefore installed on a side of a 3 positions wheel: for one of them, the fibers were facing the entrance of part of the cold optics of the instrument as shown on figure 4. Two additional fibers were installed behind a hole in a mirror facing the focal plane and illuminating all the bolometers synchronously, for time constant measurements. Being further from the instrument, the mirror fibers illuminate HFI horns about 300 times less than the wheel fibers.

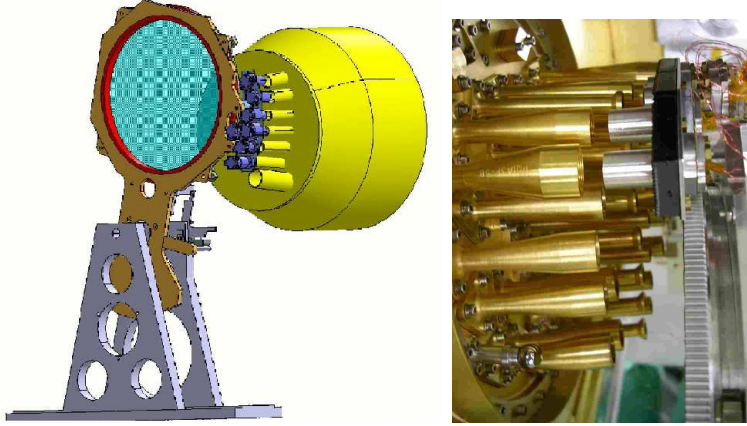


Figure 4: Schematics and picture of the setup used for the characterisation of the Planck-HFI instrument (which cold optics is represented in yellow on the left and which is in gold on the picture) with the carbon fibers illuminators (resp. in blue and in grey).

4 Characterisation

4.1 Resistance and temperature

At room temperature the measured resistivity of the fibers is $1.8 \cdot 10^{-5} \Omega \cdot m$ which gives for 1mm fibers a resistance of 640 Ohms at 300K. This resistance does depend on the thermalisation temperature as shown on figure 5 for seven fibers (on the left): the dispersion of these measurements includes the spread of the resistance of the Ag-lacquer contacts and the fact that the length of the fibers lies between 0.94 and 1.06 mm. The figure on the right shows, for the same seven fibers, their resistance corrected for their value measured at 80K and divided by the slope $\frac{dR}{dT}$ at $T = 80K$ to correct for length effects. It illustrates the homogeneity of the results. The contact resistance due to the Carbon-Ag lacquer interfaces is of the order of 100Ω.

4.2 Thermal conductivity

We measure and check the thermal conductivity κ using the two experimental setups described in section 3.

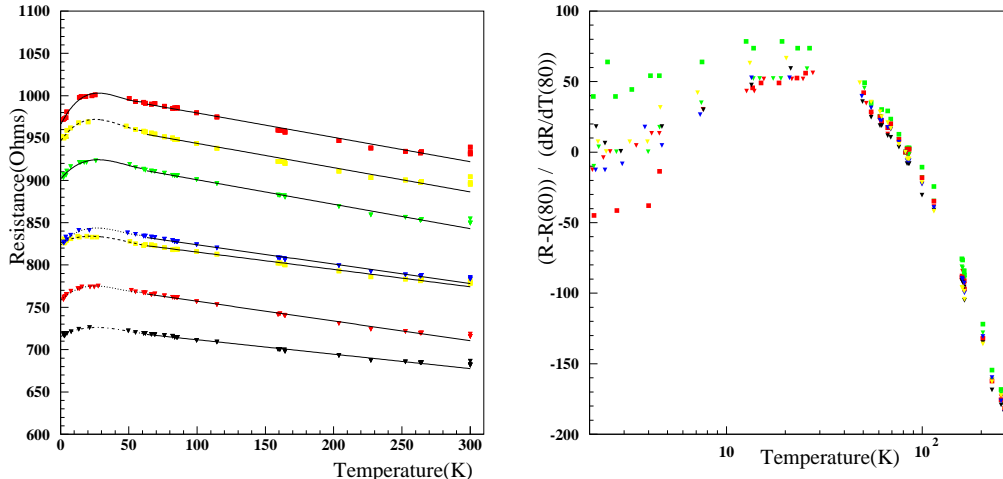


Figure 5: On the left: resistance of the fibers as a function of the thermalisation temperature (a polynomial fit is superimposed). On the right: comparison of the same data when properly normalized (cf. text).

4.2.1 With the dedicated electronics

The first step of the analysis using the dedicated electronics is to estimate the resistance variation of the fibers as a function of the thermalisation temperature for very small voltages applied on their edges (typically under 100mV), heating the fiber about $10K$ above T_0 . For such a voltage V_a , we measure the amplitude V_f of the signal between $t = 0$ and its asymptotic value, and the difference ΔV_r of the voltage signals measured at the edges of the same fiber when pulsed in series with the resistance $r = 2.65\Omega$ and without r (cf. Figure 3). The variation of the resistance induced by a tension V_a applied on the fibers is given by:

$$\Delta R_a = \frac{V_f}{\Delta V_r} r \quad (12)$$

We deduce the value of the mean temperature to which the fiber is heated inverting the polynomial function used to fit the $R(T)$ behaviour of the fibers presented in section 4.1. For instance, above 40K, the resistance is propor-

tional to the temperature (cf. section 4.1) and one gets from (4) and (8):

$$\kappa = -\frac{V_a^2 L \alpha}{12 S \Delta R_a} \quad (13)$$

The results are shown on figure 6 for seven superimposed fibers. κ is well described in this temperature range by the parametrisation:

$$\kappa = \kappa_0 + \kappa_2 T^2 + \kappa_3 T^3 \quad (14)$$

the full line curve corresponds to a fit of data with:

$\kappa_0 \simeq 0.3 \pm 0.1 \text{W/Km}$, $\kappa_2 \simeq (2.5 \pm 0.8) 10^{-4} \text{W/K}^3 \text{m}$, and $\kappa_3 \simeq (-5. \pm 3.) 10^{-7} \text{W/K}^5 \text{m}$.

These results are in good agreement with other measurements on carbon fibers[5].

The small slope of $\kappa(T)$ at low temperature makes the fiber signal very stable even if T_0 is not stabilized. For instance, with T_0 around 4K with variation of the order of 100mK , the fiber signal varies by less than 10^{-3} .

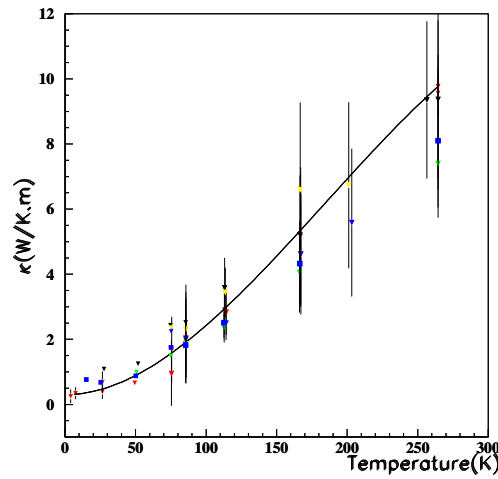


Figure 6: Thermal conductivity κ as a function of the temperature for seven Carbon fibers. The full line corresponds to a fit according to eq. (14)

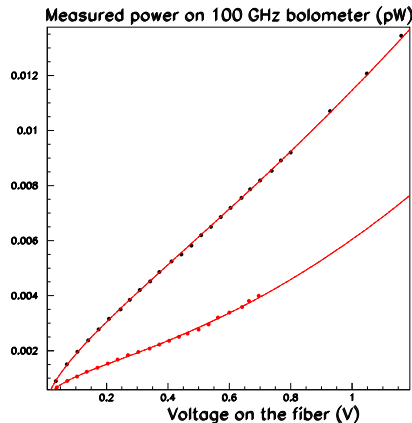


Figure 7: Incident power measured by a 100GHz Planck-HFI bolometer (in pW) - without corrections for optical efficiency of the cold optics of the instrument - as a function of the voltage applied at the edges of the fibers for 2 different fibers: a 1mm length fiber (in black) and a 0.6mm one (in red). The superimposed fitted function corresponds to the parameterization given in equation (17).

4.2.2 Bolometers data

In order to cross-check this result, one makes use of the Planck HFI instrument. We pulse the fibers with square signals at approximately 1 Hz , and compute the amplitude S_{bolo} of the resulting synchronous signal measured on the bolometers (translated in terms of incident power on the detectors). S_{bolo} is proportional to the integral of the temperature increase over the length of the fiber⁴. Table 1 gives the measured values of the flux (in pW) with the bolometers for the fibers installed on the mirror and pulsed with 1V amplitude signals⁵.

Figure 7 shows the power measured by one of the bolometers (at 100GHz) for two “mirror” fibers (a small 0.6mm fiber and a longer 1mm one) as a function of the voltage applied on the fiber.

⁴One assumes that, being in the Rayleigh Jeans domain, the emission spectrum of the fiber is proportional to T .

⁵These values have to be multiplied by a factor 350 if one wants to estimate the flux when the fiber is directly facing the entrance of the horn of the cold optics in front of the bolometers.

	100GHz	143 GHz	217 GHz	353GHz	545 GHz
Flux(10^{-3} pW)	11.	10.	21.	117.	27.

Table 1: Measured flux for each Planck-HFI frequency band for the fibers installed on the mirror and pulsed with 1V amplitude signals.

These results can be understood in the light of the framework given in section 2. In the permanent regime, using (14) to parametrize $\kappa(T)$ and neglecting $R(T)$ dependence, one gets from equation (1):

$$\frac{\partial^2}{\partial x^2} \left(\kappa_0 T + \frac{\kappa_2 T^3}{3} + \frac{\kappa_3 T^4}{4} \right) = -\frac{V^2}{LSR}. \quad (15)$$

Since $T = T_0$ for $x = \pm L/2$, one obtains after integration:

$$\kappa_0 T(x) + \frac{\kappa_2}{3} T^3(x) + \frac{\kappa_3}{4} T^4(x) = A(x) + \gamma \quad (16)$$

where:

$$A(x) = \frac{V^2}{2LSR}(L^2/4 - x^2), \text{ and } \gamma = \kappa_0 T_0 + \frac{\kappa_2}{3} T_0^3 + \frac{\kappa_3}{4} T_0^4.$$

Since here $T_0 \approx 2K$, it can be neglected with respect to T . Hence, $\gamma = 0$.

$A(x)$ simplifies to $A(x) = V^2/(8\mu)(1 - (2x/L)^2)$. Hence, the solution $T(x)$ is only a function of V and the reduced variable $\xi = 2x/L$.

For small V values, the first term dominates the left-hand side of (16), that reduces to (3), and $T(x)$ has a parabolic shape. At medium V values, $T(x)$ solution on most part of the fiber implies mainly the T^3 term, and $T(x)$ has a flatter profile with a $\sqrt[3]{1 - \xi}$ shape.

At high V value, the negative κ_3 term plays a higher role and is responsible for the increase in the $T(x)$ slope.

The phenomenological expression:

$$S_{bolo} \propto G_0 V^2 + \frac{G_2}{3} V^{2/3} + \frac{G_3}{4} V^{1/2} \quad (17)$$

is found to fit accurately both experimental (see figure 7) and simulated data (see section 5).

Here, the applied voltages are higher than the ones used in the previous section, still the model fits accurately the data and both results are in very good agreement.

4.3 Time constants and Calorific capacitance

With the dedicated electronics of section (3.1), and applying only small voltages to the fibers, one can extract the fiber time constant by fitting the exponential behaviour of $V_1(t)$ in a wide range of thermalisation temperature T_0 . The results on τ are illustrated on figure 8: on the left hand side the data are in ms while on the right there are normalized to the mean value obtained for each fiber with $T \geq 250K$, showing that this behaviour is coherent from one fiber to the others.

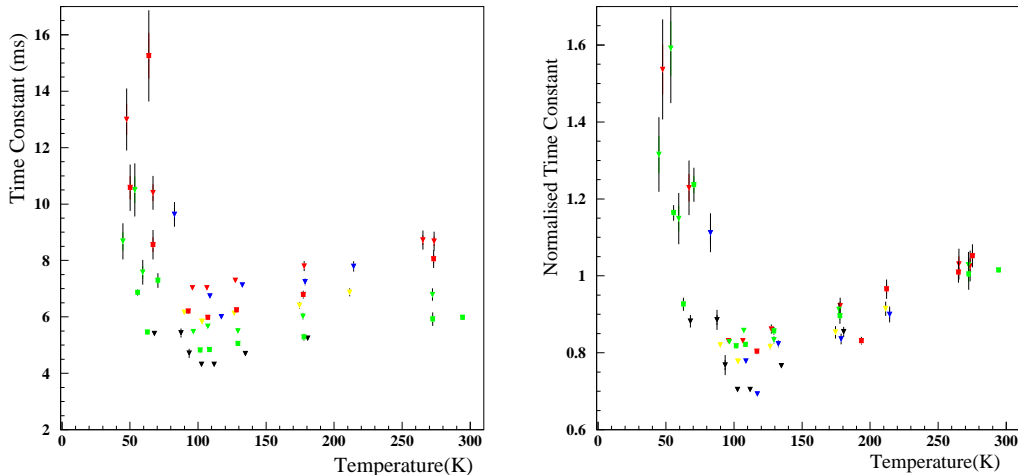


Figure 8: On the left: Time constant (in ms) as a function of the thermalisation temperature. On the right: same data but normalized to the mean value obtained for each fiber with $T \geq 250K$.

In the temperature range we explore, the fiber time constants present a minimum around $100K$, and rise slowly up to $300K$. The higher time constants measured for a temperature smaller than $50K$ are responsible for long decay times at the end of the pulse. During the Planck HFI calibration [3], this drawback has been corrected for using a small permanent current on the fiber in addition to the pulse. This permanent current allows to maintain most of the fiber at temperatures where the time constant remains small, and we recover a fiber decay time in the same range as the rise time.

C_p can be deduced from the measurement of the time constant and from the κ modelisation through relation (7). Figure 9 shows individual results

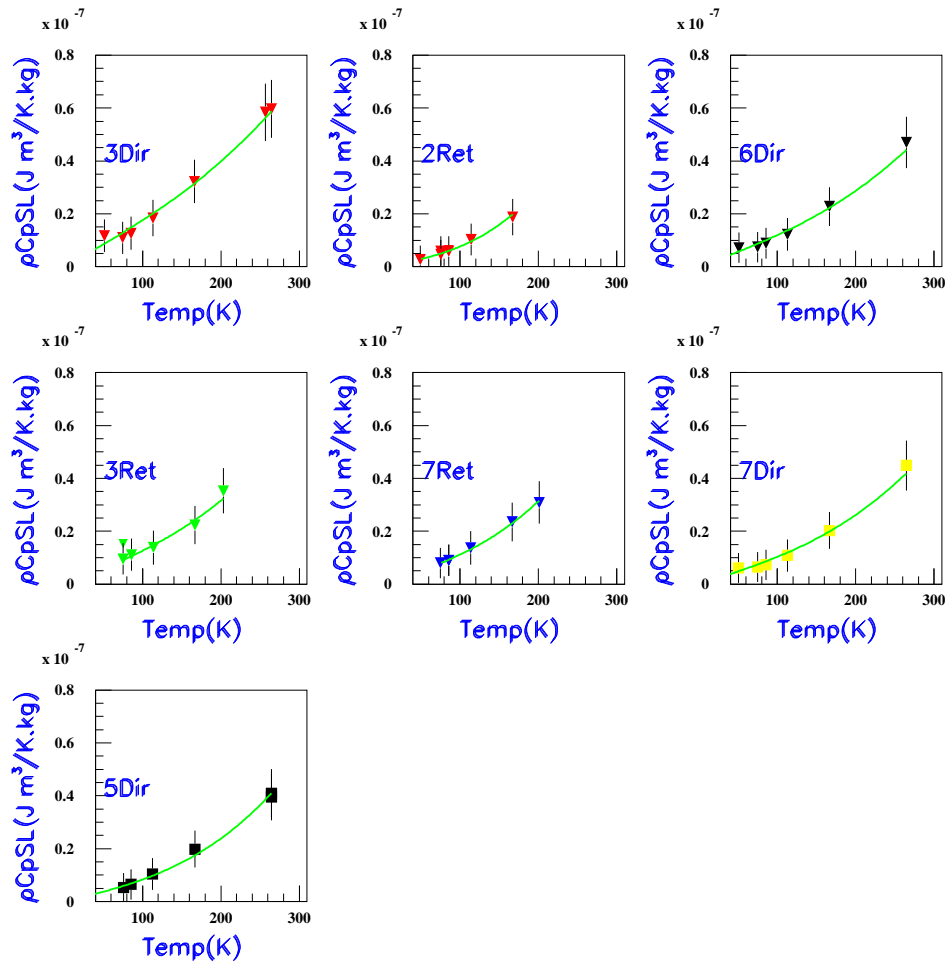


Figure 9: Calorific capacitance C_p as a function of the temperature for several Carbon fibers.

for seven fiber calorific capacitance. Parametric adjustments of the standard type $C_p/T = C_{p0} + T^2 C_{p2}$ are superimposed. A good qualitative agreement is met with expected values for Carbon fiber at low temperature[6].

5 Simulation

We developed a simple simulation code solving numerically equation 1. Using the Crank Nicholson scheme [7] and introducing the fitted dependence on the temperature of R , κ and C_p , we can compute the behaviour of the mean temperature of the fiber as a function of the input voltage: it is shown on figure 10 which reproduces the results measured on the bolometers (cf. Figure 7). The parameters extracted from data with some approximations are therefore coherent with the simulations.

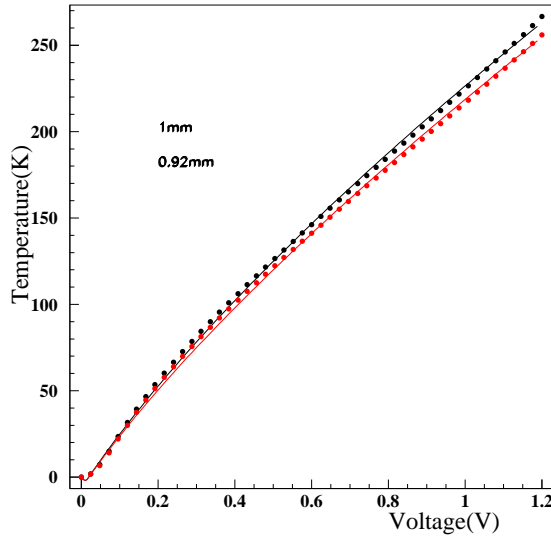


Figure 10: Simulation of the mean temperature of the fiber as a function of the amplitude of the applied voltage for several fibers lengths.

6 Conclusion

This article describes the physical parameters of the carbon fiber illuminators used in the calibration of the Planck-HFI instrument. We have shown that, thanks to their low time constant ($\leq 10ms$ for 1mm fibers at 2K), they can be used in a pulsed regime without introducing any electrical parasitic signal on HFI's bolometers, and that their emission spectrum gives a significant amount of signal in the submm domain.

We have detailed an analysis of the temperature dependence of the resistance, the calorific capacitance C_p , and the thermal conductivity κ , of these fibers based on measurements from 300 to 1.7K. We end up showing the good agreement between simulations of the 1D heat equations making use of the extracted parameters ($R(T)$, $C_p(T)$ and $\kappa(T)$) and data measured of the 100mK HFI's bolometers.

This well understood picture of the fibers behaviour makes them a very usefull tool for FIR instrument calibration.

Acknowledgments: We wish to aknowledge J.C. Vanel and C. Rosset for their help in our first attempt to cool down the fibers, B. Maffei and R. Sudiwala for providing us with material and manpower at Cardiff, J.P. Torre for his disponibility and his setup, O. Perdereau, J. Haissinski and S. Plaszczyński for usefull discussions and help, and F. Pajot, P. Lami and the Saturne Cryostat team for the Planck-HFI calibration.

This work has been funded by CNES as part of LAL contribution to HFI, under contract N 737/CNES/01/8961/00.

References

- [1] Planck. The Scientific Programme - ESA-SCI(2005)1
N. Mandolesi et al, "the ESA Medium Size Mission for measurements of CBR anisotropy", Planet. & Space Sci.,1995, 43, 10/11, pp. 1459.
- [2] J.M. Lamarre et al., "The Planck High Frequency Instrument, a third generation CMB experiment, and a full sky submillimeter survey", 2003, New Astronomy Reviews, Volume 47, Issue 11-12, p. 1017-1024.
- [3] F. Pajot et al., "HFI Calibration Plan"; 30/01/2002; Edition: 3, Revision: 0, PL-PHZW-100061-IAS. This report is qualified as "Public".

- [4] Habilitation à diriger des recherches Henrot-Versillé S., "Archeops et Planck-HFI : Etudes des systématiques pour l'analyse du fond diffus cosmologique", Université Paris Sud - Paris XI <http://tel.archives-ouvertes.fr/tel-00102694/en/>
- [5] J. Heremans et al., Thermal conductivity and Raman spectra of carbon fibers, *Phys. Rev. B*, **32**, 10 (1985)
- [6] C. Pradère et al., Specific-heat measurement of single metallic, carbon, and ceramic fibers at very high temperature, *Rev. of Sci. Instr.* **76**, 064901 (2005).
- [7] See, e.g., W. H. Press, S. A. Teukolsky, W. T. Vetterling, and B. P. Flannery, *Numerical Recipes in Fortran 77*, 2nd. ed. Cambridge University Press, Cambridge, England, 1992, Sec. 19.2.